High-resolution density assessment assisted by deep learning of *Dendrophyllia cornigera* (Lamarck, 1816) and *Phakellia ventilabrum* (Linnaeus, 1767) in rocky circalittoral shelf of Bay of Biscay

Alberto Gayá-Vilar [1] , **Adolfo Cobo** [2] , **Alberto Abad-Uribarren** [3] , **Augusto Rodríguez** [3] , **Sergio Sierra** [4] , **Sabrina Clemente** [1] , **Elena Prado** [Corresp. 3]

[1] Department of Animal Biology, Soil and Geology, University of La Laguna, San Cristóbal de La Laguna, Santa Cruz de Tenerife, Spain

[2] Photonics Engineering Group, University of Cantabria, Santander, Cantabria, Spain

[3] Santander Oceanographic Center, Spanish Institute of Oceanography (IEO-CSIC), Santander, Cantabria, Spain

[4] Complutum Geographic Information Technologies (COMPLUTIG), Alcalá de Henares, Madrid, Spain

Corresponding Author: Elena Prado
Email address: elena.prado@ieo.csic.es

This study presents a novel approach to high-resolution density distribution mapping of two key species of the 1170 “Reefs” habitat, *Dendrophyllia cornigera* and *Phakellia ventilabrum*, in the Bay of Biscay using deep learning models. The main objective of this study was to establish a pipeline based on deep learning models to extract species density data from raw images obtained by a remotely operated towed vehicle (ROTV). Different object detection models were evaluated and compared in various shelf zones at the head of submarine canyon systems using metrics such as precision, recall, and F1 score. The best-performing model, YOLOv8, was selected for generating density maps of the two species at a high spatial resolution. The study also generated synthetic images to augment the training data and assess the generalization capacity of the models. The proposed approach provides a cost-effective and non-invasive method for monitoring and assessing the status of these important reef-building species and their habitats. The results have important implications for the management and protection of the 1170 habitat in Spain and other marine ecosystems worldwide. These results highlight the potential of deep learning to improve efficiency and accuracy in monitoring vulnerable marine ecosystems, allowing informed decisions to be made that can have a positive impact on marine conservation.

High-resolution density assessment assisted by deep learning of *Dendrophyllia cornigera* (Lamarck, 1816) and *Phakellia ventilabrum* (Linnaeus, 1767) in rocky circalittoral shelf of Bay of Biscay

Alberto Gayá-Vilar[1], Adolfo Cobo[2], Aberto Abad-Uribarren[3], Augusto Rodríguez-Basalo[3], Sergio Sierra[4], Sabrina Clemente[1], Elena Prado[3]

[1]Department of Animal Biology, Soil and Geology, University of La Laguna, San Cristóbal de La Laguna, Santa Cruz de Tenerife, Spain
[2]Photonics Engineering Group, University of Cantabria, Santander, Cantabria, Spain
[3]Santander Oceanographic Center, Spanish Institute of Oceanography (IEO-CSIC), Santander, Cantabria, Spain
[4]Complutum Geographic Information Technologies (COMPLUTIG), Alcalá de Henares, Madrid, Spain

Elena Prado
Av. de Severiano Ballesteros, 16, 39004 Santander, Cantabria, Spain
Email address: elena.prado@ieo.csic.es

Abstract

This study presents a novel approach to high-resolution density distribution mapping of two key species of the 1170 “Reefs” habitat, *Dendrophyllia cornigera* and *Phakellia ventilabrum*, in the Bay of Biscay using deep learning models. The main objective of this study was to establish a pipeline based on deep learning models to extract species density data from raw images obtained by a remotely operated towed vehicle (ROTV). Different object detection models were evaluated and compared in various shelf zones at the head of submarine canyon systems using metrics such as precision, recall, and F1 score. The best-performing model, YOLOv8, was selected for generating density maps of the two species at a high spatial resolution. The study also generated synthetic images to augment the training data and assess the generalization capacity of the models. The proposed approach provides a cost-effective and non-invasive method for monitoring and assessing the status of these important reef-building species and their habitats. The results have important implications for the management and protection of the 1170 habitat in Spain and other marine ecosystems worldwide. These results highlight the potential of deep learning to improve efficiency and accuracy in monitoring vulnerable marine ecosystems, allowing informed decisions to be made that can have a positive impact on marine conservation.

Keywords: Artificial Intelligence, Vulnerable Marine Ecosystem, Habitat Mapping, Object Detection Model, Natura 2000 Network

Introduction

The Habitats Directive (Directive 92/43/EEC) establishes the "Natura 2000" network, a network of European sites which aims to maintain or, if possible, re-establish a favorable conservation status for certain types of natural habitats and certain animal and plant species. The marine Natura 2000 network is an integral part of the European ecological network Natura 2000, and constitutes the application of the Habitats Directive and the Birds Directive (Directive 2009/147/EC) in the marine environment, considered the two most important legislative tools for the conservation of biodiversity in Europe. The Natura 2000 network is composed of Sites of Community Importance (SCI), which eventually become Special Areas of Conservation (SAC), and Special Protection Areas for Birds (SPA).

The Habitats Directive (92/43/EEC) lists different types of marine habitats that are important for the community and need to be conserved. To do this, Special Areas of Conservation (SACs) are designated. One of the habitats listed in Annex I of the Habitats Directive is Habitat 1170, which refers to Reefs. Reefs in the sense of the Directive are considered to be all those compact hard substrates that outcrop on the seabed in the sublittoral (submerged) or littoral (intertidal) zone, whether of biogenic or geological origin.

In Spain, the Habitat 1170 Reefs extends along the entire coastline and marine waters, from coastal areas to the deep seabed, occupying extensive regions. In this diverse array of Habitat 1170 typologies, our focus narrows to two rocky outcrops within the Cantabrian Sea's circalittoral shelf. These outcrops are categorized as vulnerable marine ecosystems (VMEs) due to their importance as biodiversity hotspots and ecosystem functioning in the deep sea (FAO, 2009). Circalittoral rocky substrates, located within the phytal system below the maximum distribution level of marine phanerogams and photophilic algae, and extending to the scyaphilic algae's maximum depth, are characterized by low light levels and relatively stable hydrodynamic conditions compared to shallower regions.. The depth at which the circalittoral zone begins depends directly on the amount of light penetrating the seafloor. Animal species predominantly dominate most circalittoral rocky substrates due to the diminished light conditions. The number of species living on these seabeds can be very highly variable, influenced by geographical factors, seabed geomorphology, and various environmental elements (Dominguez-Carrió et al., 2022).

Within the Cantabrian circalittoral rocky platform, communities consist mainly of numerous sponge and coralligenous species, which provide three-dimensional structure to these habitats, classifying them under Habitat 1170 Reefs. However, despite their importance as structuring species, their small size and highly fractionated distribution of this organism on the seabed pose significant challenges for mapping . Simultaneously, monitoring these species and tracking community distribution across time and space is imperative for habitat protection. The use of remotely operated vehicles (ROV's) imagery has emerged as a valuable tool to address this challenge.

Underwater vehicles generates a large amount of in situ, non-destructive, representative and potentially repeatable samples, and this allows not only a complete characterization of benthic diversity but could also lay the groundwork for a long-term monitoring initiatives (Dominguez-Carrió et al., 2022). However, processing this information has encountered bottlenecks, primarily attributed to the time-consuming, labor-intensive and costly nature of annotating visual data (Weinstein, 2017). In addition, deep ecosystems present complex environments characterized by unbalanced light conditions, low contrast, and the presence of occlusion and organisms camouflage. Under these circumstances, objects captured by the ROV camera become challenging to identify (Song et al., 2022).

To address these problems and obtain quantitative information from underwater images, new automated image analysis tools have emerged. One of the most promising approaches involves the use of deep learning techniques based on neural networks, a combination of artificial intelligence and computer vision. This approach entails the application of multiple layers of highly interconnected machine learning algorithms to achieve improved results from raw images (Olden et al., 2008; Le Cun et al., 2015). These techniques have already achieved formidable results in different marine ecology tasks such as coral classification (Bhandarkar et al., 2022; Mahmood et al., 2017; Raphael et al., 2020), fish detection and classification (Zhong et al., 2022; Siddiqui et al., 2018; Knausgård et al., 2021), and identification of diverse benthic fauna (Abad-Uribarren et al., 2022; Song et al., 2022; Liu & Wang 2022).

Within the field of deep learning, object detectors can be classified into two categories: two-stage detectors and single-stage detectors. Two-stage detectors exemplified by Faster R-CNN (Ren et al., 2017), first generates a set of region proposals (RPN) before determining the object category and location. In contrast, single-stage detectors, such as YOLO (Redmon et al., 2016), simultaneously identify and locate objects in a single step. These object detection models can be used as tools to automate species identification procedures and generate accurate density maps for ecosystem monitoring. Surveys employing these models yield comprehensive records of ecosystems and facilitate the identification of trends in habitat health and biodiversity.

Marine ecosystems are subject to numerous threats and impacts, such as climate change, waste pollution, commercial fishing and deep sea mining (Pinheiro et al., 2023). Therefore, it is important to generate detailed mapping of their most vulnerable ecosystems in order to make informed decisions about their management and conservation. Accurate mapping facilitates the identification of critical areas that require protection and the development of effective strategies to mitigate negative impacts on the ecosystem (Rodriguez-Basalo et al., 2022).

In this study, we assess the density of Habitat 1170 structuring species in two circalittoral rocky shelf areas of the Cantabrian Sea. We employ object detection models to automatically identify and label species in underwater images. Initially, we compare object detection models with different neural architectures, to determine the most effective model for generating species density maps from geolocated images obtained along a photo-transect. Subsequently, the model demonstrating the best metrics is employed to establish a pipeline for generating detailed species density maps. Our ultimate goal is to create an initial base map for monitoring ecosystem health, offering a comprehensive geographic description of Habitat 1170 structuring species, and serving as a support tool for decision-making in Natura 2000 network areas. The expected results of this model's application include the automated generation of density and geographic presence data for benthic species *D. cornigera* and *P. ventilabrum*, with results presented through species density maps.

Materials and methods

Study area

The research was centered on two rocky outcrops situated within the circalittoral shelf of the Aviles submarine Canyons System (ACS)and the Capbreton submarine Canyons System (CCS), both located in the Cantabrian Sea to the south of the Bay of Biscay (Figure 1). The ACS has been designated as a Site of Community Interest (SCI) and is currently undergoing studies aimed at elevating its status from SCI to Special Area of Conservation (SAC).Likewise, the CCS area is under examination for SCI status, with the intention of integrating it into the marine Natura 2000 Network.

These studies are part of the actions carried out in the LIFE IP INTEMARES project (Baena et al., 2021).

In the Bay of Biscay, the continental shelf is generally narrow, a common feature of compressive continental margins (Ercilla et al., 2008). The region is characterized by the presence of rocky outcrops mainly formed due to sedimentary transport mechanisms associated with oceanographic dynamics. These rocky outcrops serve as critical habitats for a diverse array of benthic communities, many of which fall within the 1170 habitat category.forming a heterogeneous and complex ecosystem capable of supporting a rich biodiversity. . Within these communities, our study focuses on two species selected for their significant role in structuring the 1170 habitat within the rocky circalittoral platform of the Cantabrian Sea (Rodríguez-Basalo et al., 2022). These species are the yellow coral *Dendrophyllia cornigera* (Lamarck, 1816) and the cup sponge *Phakellia ventilabrum* (Linnaeus, 1767) (Figure 2).

ROTV underwater imagery

High-resolution underwater images obtained using the remotely operated towed vehicle (ROTV) Politolana (Sánchez & Rodríguez, 2013) were employed. The ROTV Politolana, designed by the Santander Oceanographic Center of the Spanish Institute of Oceanography (IEO-CSIC), has the capability to descend to a maximum depth of 2000 m. For seabed exploration, the ROTV Politolana uses photogrammetric methods and is equipped with a high-resolution camera, bidirectional telemetry and an acoustic positioning system. Additionally, the vehicle is equipped with four laser pointers coupled at a precise distance of 25 cm from each other. This configuration allows precise measurements and detailed data to be obtained during each deployment. Furthermore, the vehicle acquires high-definition images and videos synchronized with environmental data, ensuring the acquisition of comprehensive datasets during each dive.

In total, 20 transects were conducted for this study, with an average length of 410 m per transect. In the ACS, images were acquired during the INTEMARES A4 Avilés oceanographic campaign (2017). In contrast, in the CCS, photographic transects were carried out during the INTEMARES-Capbreton 0619 and 0620 campaigns (2019 and 2020). These transects, both in ACS and CCS, were carried out in a depth range between 90 and 300 m.

The Politolana ROTV captures photographs at time intervals ranging from 0.5 s and 20 s, depending on the chosen sampling configuration. This approach provided representative data of the habitat and benthic communities to be characterized.

These high resolution images provided comprehensive views of the seafloor in (Figure 3). In total, 5012 images were contributed from both ACS and CCS for this study.

Image preprocessing and algorithm training

To evaluate the model's generalization capabilities, 60 images from a pool of 300 obtained from the ACS were randomly selected as the validation set. The remaining 240 images were used as training images in a ratio of 8 to 2. Ensuring that there were no repeated images or individuals between the training and validation sets was crucial to prevent model overfitting.

For image annotation, we utilized the Supervisely image data annotation software (https://supervise.ly/), enabling the creation of bounding boxes around the target species *D. cornigera* and *P. ventilabrum*. Our labeling approach ensured that each annotation encompassed the entire individual while minimizing background area (Figure 4). The training data set received meticulous attention, with 527 and 1045 annotations performed for the *D. cornigera* and *P. ventilabrum* classes. Annotations were carried out by trained expert scientists. To balance class distribution, the Supervisely flying object function (https://github.com/supervisely-ecosystem/flying-objects) was used. This function generates synthetic data for object detection tasks. Specifically, it involved annotating specimens from both classes as masks, followed by the application of magnifications to the objects and their distribution on different selected backgrounds. With the creation of 20 synthetic images, class balance was achieved with 2330 and 2605 annotations for the classes *D. cornigera* and *P. ventilabrum*, respectively (Figure 4).

In addition, to evaluate the capacity of the model to generalize across varying environmental conditions 60 images were randomly selected from the CCS area, a region where the two target species are exposed to different environmental pressures. These images were used as validation images to determine if the model was able to correctly detect the target species.

All object detection models were based on the same pre-training weights from the COCO (Common Objects in Context) dataset, which is a widely used dataset in computer vision research. The models were trained on selected ACS images, both with and without data augmentation. The training spanned 200 epochs, allowing the models to continually improve their accuracy and performance. During each epoch, the models processed the entire training data set, iteratively adjusting their parameters to minimize prediction error. This allowed the models to continuously improve their ability to accurately detect the target species.

Automatic species labeling of underwater images using deep learning

For automatic annotation of the image set, a deep learning based framework was developed, considering three different deep neural network architectures. A neural network consists of input layers that receive the data, a processing core with hidden layers, and output layers that provide the model output. The term "deep" refers to the number of hidden layers in the neural network structure. A neural network is trained to produce the desired output by adjusting its internal parameters, called weights, based on the error between the model output and the correct response. This adjustment is performed by a process called gradient descent (Schmidhuber, 2014).

This study compared, three object detection models with different neural architectures: YOLOv7 and YOLOv8 (Bochkovskiy et al., 2022; Karmaker et al., 2023), both single-stage models, and Faster R-CNN (Ren et al., 2017), a two-stage model. YOLO single-stage models have been shown to have advantages compared to Faster R-CNN (Abdulghani & Menekşe Dalveren 2022; Maity et al., 2021; Zheng et al., 2022), so the latter two model versions were included in the comparison.

YOLOv7 and YOLOv8 are real-time object detection models that employ convolutional neural networks (CNNs) to efficiently identify and localize objects in images. YOLOv7 uses the ELAN architecture, which improves the learning and convergence capabilities of deep networks. On the other hand, YOLOv8 integrates advances in deep learning and computer vision, including attention structures and dilation convolution blocks, resulting in improved speed and accuracy in object detection. In this study, the YOLOv8x model was used for YOLOv8 training, while the YOLOv7-E6E model was used for YOLOv7 training.

Faster R-CNN, a two-stage object detection model, integrates a CNN for features extraction and a Region Proposal Network (RPN) to generate high-quality proposals. The RPN predicts the boundaries and objectivity scores at each image position and is trained end-to-end. These proposals are then used by Faster R-CNN in the object detection and classification stage (Ren et al., 2017). In this study, the X-101-32x8d model was used for Faster R-CNN training.

The YOLOv8x, YOLOv7-E6E and Faster R-CNN X-101-32x8d versions were chosen for this study because of their object detection performance. According to the data and the information available in the GitHub repositories, these versions present high performance in terms of accuracy and speed in object detection.

For training the object detection models, we used Google Colab Pro, a platform that provided us access to the NVIDIA A100-SXM GPU. This high-performance GPU enabled efficient processing of large datasets and expedited model training. Furthermore, Google Colab facilitated seamless code sharing and result dissemination among team members.

Object detection model selection

To evaluate the performance of the different models in the task of detecting *D. cornigera* and *P. Ventilabrum* within the ACS and CCS shelf areas, we selected three widely used metrics for object detection tasks: precision, recall, and F1 Score. These metrics were compared and analyzed for the YOLOv8, YOLOv7, and Faster R-CNN object detection models.

Precision measures the accuracy of the model predictions, representing the percentage of predictions that are correct.

Recall (or the sensitivity of a classifier) evaluates how effectively the model identifies all positive instances, quantifying the number of actual positives correctly labeled as positives.

The F1 score serves as an index that evaluates the balance between precision and recall, a widely used metric in deep learning for comparing the performance of two models on the same task. The calculations for precision, recall and F1 are described by the following equations (1), (2) and (3) (Van Rijsbergen, 1974):

$$\text{precision} = \frac{\text{True positives}}{\text{True positives} + \text{False positives}} \quad (1)$$

$$\text{recall} = \frac{\text{True positives}}{\text{True positives} + \text{False negatives}} \quad (2)$$

$$F1 = 2 \cdot \frac{\text{precision} \cdot \text{recall}}{\text{precision} + \text{recall}} \quad (3)$$

For model evaluation, an intersection over union (IoU) of 0.5 was adopted. IoU quantifies the overlap between the detection and the actual object, calculated as the intersection between the two bounding boxes divided by their union (Figure 5). An

IoU of 0.5 implies that 50% of the area of the real object's area is covered by the detection. In addition, metrics were computed for two different confidence thresholds (0.5 and 0.6), enabling assessment of the model's detection performance at different levels of certainty.

Both Aviles training datasets, with and without augmentations, were used for evaluating the models on the Aviles and Capbreton validation datasets. The addition of the Capbreton dataset was crucial for assessing the model`s ability to generalize to other canyon systems subjected to different pressures and environmental conditions.A comprehensive evaluation of the models was conducted under different scenarios and conditions, ensuring the acquisition of accurate and reliable results for object detection in subsea systems.

Pipeline for species density map generation

To streamline the process of generating species density maps from raw transect images, A pipeline was implemented in Google Colab Pro (Figure 6). The images were synchronized with the ROTV telemetry data, which provided information on the depth, coordinates, and height of the ROTV relative to the seafloor for each transect image. In parallel, using ImageJ software (version 1.53o), the distance between the ROTV laser pointer marks on 50 images was manually measured to obtain the area covered by each image based on its resolution. With this data, a simple regression model was trained using machine learning techniques to relate the area to the height of the ROTV relative to the seafloor. The model predictions were used to calculate the area of the rest of the images.

Simultaneously, predictions were carried out using the YOLOv8 model, previously trained with our data (YOLOv8-SCS), to analyze the images captured in the transects. Notably, in the comparison of object detection models, YOLOv8 obtained the best metrics with an IoU of 0.5 and a confidence threshold of 0.6 (Figure 7). Therefore, we set these parameters to perform the predictions and generate the inferences in the workflow. These results were integrated with the area and coordinates of each image in order to calculate the number of individuals per square meter in each image.

Finally, QGIS software (version 3.22) was used to create maps based on the species density data obtained from each transect image point. We applied a symbology scheme based on graduated symbol sizes to represent density categories (Schmidt et al., 2022). The density data series was classified into intervals according to their values, and each interval was assigned a corresponding symbol size, with larger sizes indicating higher densities. This approach facilitated the clear visualization of areas with the highest species density on the generated maps.

Results

Comparison of object detection models

In the evaluation of object detection models, we compared one-stage models YOLOv7 and YOLOv8 with the two-stage model Faster R-CNN. Our assessment included both models trained with and without data augmentation, and the results are summarized in Table 1. Notably, data augmentation significantly improved the performance of all three models, with the one-stage models demonstrating more substantial enhancements for *D. cornigera*. YOLOv8 achieved a recall rate of 18.5% and an F1 score of 11.4%, while YOLOv7 showed improvements above 7.7% across all its metrics. For *P. ventilabrum* species, the Faster R-CNN model showed the most significant improvement with an 8.5% increase in recall and a 5.2% in F1 score. The YOLOv8 model also showed a 5.7% improvement in precision.for *P. ventilabrum*.

Figure 7 provides a comparison of metrics for detecting *P. ventilabrum* and *D. cornigera* species using the YOLOv8, YOLOv7, and Faster R-CNN models in both the ACS and CCS regions. The analysis includes augmented data and confidence thresholds of 0.5 and 0.6. Notably, the YOLOv8 model outperforms the other models in terms of precision, recall, and F1 for both confidence thresholds. In the ACS, the YOLOv8 model achieves precision values exceeding 92.3% for P. ventilabrum and exceptional results for D. cornigera, with a precision of 92.4%, a recall of 91.0%, and an F1 score of 91.7% for a threshold of 0.6. Furthermore, YOLOv8 exhibits superior generalization capabilities by delivering the best metrics for both species in the CCS area.

Overall, the performance of all three models improves as the threshold is increased from 0.5 to 0.6 in terms of precision and F1. These results indicate that the YOLOv8 model is most suitable for the task and a threshold of 0.6 enhances precision and F1 scores.

Figure 8 presents a visual representation of the detection results obtained using the YOLOv8, Faster R-CNN and YOLOv7 models. A detector confidence threshold was set at 0.6 and an IoU threshold at 0.5.

The images reveal that all three models occasionally misclassify certain sponges as *P. ventilabrum*, particularly Faster R-CNN, which exhibits more false detections, even mistaking *D. cornigera* for other sponge species. Notably, none of the models detect all *D. cornigera* specimens in the images, with YOLOv7 showing the highest number of undetected specimens, missing over 60% of them. YOLOv8 stands out for its ability to detect smaller *D. cornigera* specimens at high densities.

In a separate set of images, Faster R-CNN misclassifies a complex sponge as both *D. cornigera* and *P. ventilabrum* and also inaccurately identifies encrusting sponge specimens as *D. cornigera.* The YOLO-based models struggle to detect *P. ventilabrum* specimens accurately.

Overall, these results demonstrate that YOLOv8 exhibits superior detection efficiency and counting precision compared to other evaluated models, making it the preferred algorithm for detecting these valuable marine benthic species.

Species density survey

A total of 5021 transect images were processed through a pipeline designed for automatic detection of target species. These transects covered an area of 5647.48 m², with an average area covered of 282.37 m². As a result, the YOLOv8-SCS model generated 27668 automatic annotations comprising 6087 for *P. ventilabrum* and 21581 for *D. cornigera*. This resulted in an average density of 1.01 individuals/m² for *P. ventilabrum* and 3.07 individuals/m² for *D. cornigera* in the ACS and 1.18 individuals/m² for *P. ventilabrum* and 4.98 individuals/m² for *D. cornigera* in the CCS.

Species density maps were generated based on this information, allowing for a comparison of the two study areas. The CCS rocky platform exhibited the highest densities for both species, with a maximum density of 60.56 individuals/m² for *D. cornigera* and 12.96 individuals/m² for *P. ventilabrum*. These peak density observations occurred within the same transect at an average depth of 160.08 m and are illustreted in the species density maps (Figure 9).

The implementation of the YOLOv8-SCS model for automatic annotation has led to significant time savings. While a professional researcher would require approximately 210h 53min to annotate all 5021 images, the YOLOv8-SCS model accomplished the same task in just 2h 9min. This represents a time reduction of over 98%, highlighting the efficiency and effectiveness of the automatic annotation process.

Discussion

The present study addresses the need to provide efficient solutions for the monitoring, protection and conservation of vulnerable marine ecosystems (VMEs) of the circalittoral shelf by implementing automatic identification algorithms and calculating densities without human intervention. These ecosystems are crucial for maintaining marine biodiversity and play a vital role in the provision of essential ecosystem services (Ríos et al., 2022). Incorporating automatic image analysis techniques represents a significant advancement in the field of benthic community studies (Abad-Uribarren et al., 2022). The tremendous diversity of species present poses a formidable challenge for an exhaustive species analysis approach. Nevertheless, cataloging the species and their sizes provides an invaluable means to analyze community composition. Unfortunately, this aspect is frequently overlooked due to the considerable time it consumes in the evaluation process (Schoening et al., 2012). To this end, we have used deep learning tools to assist in the identification and mapping of these VMEs of rocky circalittoral shelf areas adjacent to the headwaters of two submarine canyon systems, the ACSs and CCSs. The choice of YOLOv8 as the algorithm for this task was influenced by its efficient information processing capabilities and sophisticated architecture that includes advanced loss functions (Lin, 2023). It is worth noting that various versions of the YOLO algorithms have been adapted to tackle specific challenges of underwater images, such as lack of sharpness, small size, and overlap (Zhang et al., 2022; Xu et al., 2023). The continuous evolution of these algorithms and the release of newer versions present an opportunity to test each version on the same datasets to quantify improvements in results (Zhong et al., 2022). The latest version, YOLOv8, has already shown promise in plant species recognition (Wang et al., 2023), yet its application in marine environments remains largely unexplored. This opens up new research avenues and potential enhancements to our current methodology.

Emerging from this, our study has made significant strides in the application of YOLOv8 to marine environments. Despite the inherent challenges posed by the notable morphological differences between specimens of the same species, such as the diversity in shapes, sizes, and complexity of the colonies of *D. cornigera*, and the variability in sizes and shapes of *P. ventilabrum*, YOLOv8 has proven to be highly effective. It has achieved F1 values higher than 91.7% for both species in the ACS, indicating a high level of detection precision and recall. Furthermore, it has managed to detect both species with accuracies above 92.4% in the ACS. These results not only support the study by Li et al. (2023), which concludes that YOLOv8 is a suitable model for complex conditions, showing remarkable universality and robustness in detecting objects in images with variability and noise but also contribute significantly to our understanding of rocky circalittoral shelf habitats and the distribution patterns of vulnerable species within Natura 2000 areas.

The success in detecting the species can be attributed to the prior training of the models on large-scale datasets, such as COCO (Lin et al., 2014), and data augmentation using synthetic imagery. This approach has been beneficial in addressing class imbalance and has improved the metrics. In particular, we observed an 11.4% improvement in F1, when including synthetic images, for the class *D. cornigera*. However, the generalization capacity of the models used is a crucial issue to ensure that the different studies and developments in the field of the application of Deep-learning to ecological studies can advance towards an operational stage. It is common to find generalization problems in which algorithms implemented and trained for one or two data sets do not work correctly when we change the study area or introduce species for which the algorithm has not been trained (W. Xu and S. Matzner , 2018). In this context, YOLOv8 demonstrated excellent generalization ability by performing well in CCS predictions. However, it was observed that YOLOv7 failed to generalize adequately, obtaining inferior metrics when switching to CCS. Therefore, validation with Capbreton (CCS) images was crucial to assess model overfitting and its impact on metrics. An alternative approach to improving model generalization involves augmenting the manual annotation effort. However, this method is associated with significant personnel and time costs (Weinstein et al., 2022). Although limited to the identification of the same target species, this study demonstrates the capacity of the selected and trained model for geographical generalization in the process of automatic labeling of underwater images.

The analysis carried out in this study provides valuable insights into the distribution patterns of two target species within and between our study areas. The species are not uniformly distributed, but seem to present a patchy distribution with higher or lower associated densities depending on the geographic location. This finding aligns with previous research, such as the study by Rodríguez-Basalo and colleagues in 2022 in ACS, which also observed differences in the densities of *D. cornígera* and *P. ventilabrum*.

In our study, we found that *P. ventilabrum* has densities ranging from 45.3 to 173 ind/100m², while *D. cornígera* shows densities ranging from 7.5 to 149.3ind/100m². This complex distribution pattern highlights the need for a comprehensive dataset consisting of multiple spatial images to accurately capture the nuances in species distribution. From an ecological and management perspective, understanding these density differences in our study areas is of great importance. Our work provides a detailed mapping of density variations for these species, serving as a foundation for future research into the underlying causes of these variations. These causes could be related to differences in environmental conditions between the study areas, varying levels of human influence, or a combination of both factors.

Our findings indicate that *D. cornigera* and *P. ventilabrum* have higher densities in the CCS compared to the ACS. Furthermore, the ACS displayed a more intricate but less abundant coral community, along with a higher prevalence of encrusting sponges and fewer three-dimensional sponges. These differences did impact the performance of our models in both study systems. However, it's important to note that despite these varying characteristics, our models demonstrated a high degree of accuracy and proficiency in object detection. It's worth emphasizing that the main focus of this work is the development of an automated annotation tool, and we do not provide an exhaustive ecological interpretation of the data generated by this tool. This limitation highlights the need for further research to explore the ecological implications of the observed distribution patterns of these two species in the study areas.

Once YOLOv8 was identified as the most effective model for the detection of the target species, we proceeded to automate the process of obtaining ecological data from raw images. The use of deep learning algorithms allows us to generate accurate and efficient species density maps (Figure 9). The time required to perform all image labeling using these automatic models is drastically reduced compared to the time required for this same task by experts, who must manually search and label each species present in thousands of images. Therefore, these models provide a great advantage, since they provide valuable information in a minimum amount of time for carrying out subsequent in-depth population and ecological studies, which result in the improvement of management measures applied in the ecosystems studied.

The presence of high densities of species belonging to the 1170 Reef habitat supports the need to establish regulations and sustainable management measures to preserve biodiversity in the ACS and CCS. These ecosystems are being considered for protection and conservation through their designation as SAC and SCI, thanks to the LIFE IP INTEMARES project, which is aligned with the global objective of reaching 30% of marine protected areas by 2030 under the umbrella of the Natura 2000 Network. This study demonstrates the importance of using advanced technologies to comprehensively study these complex and deep ecosystems serving as a basis for the establishment of appropriate legislative measures, supported by rigorous scientific information with a high degree of detail, in order to maintain the balance of the structure of these benthic ecosystems, of the trophic relationships they support, and to ensure the sustainability of the fisheries they support.

The implementation of a pipeline as a management and conservation tool for ACSs and CCSs provides the opportunity to monitor the densities of the shelf area study species. In addition, the pipeline has the potential to evolve and adapt to the needs of future surveys to obtain real-time data, cover a larger number of species, and provide more detailed information on the sizes of detected organisms. In addition, their ability to replicate over time will favor the monitoring of the environmental evolution of these areas or their possible response to the management measures applied. Several studies, such as Zhong et al. (2022), have successfully demonstrated the use of YOLO-based object detection models for real-time identification of marine animals, supporting the validity of the approach. For the extraction of species measurements there are promising state-of-the-art segmentation models such as the SAM model (Segment Anything Model) that would allow us to obtain the area occupied by the species in the image in real time (Kirillov et al., 2023). To ensure the accuracy of these measurements, it is essential to establish a protocol for ROV image capture that minimizes the possibility of errors, properly synchronizing the ROV data with the captured image. Likewise, it would also be interesting to expand the range of species detected (Li et al., 2022), which would expand the scope of the study and provide more detailed information on the structure of the communities in the area. This tool would provide a holistic perspective, being able to detect changes in marine life patterns in terms of density, mean sizes and biomasses, in order to properly assess the impact of human activities on these habitats. This would facilitate the adoption of measures to protect and conserve these unique marine ecosystems.

Regarding possible improvements of the present work, it is suggested to use a larger and more diverse set of high quality images to train the model. It is proven that increasing the number of images during training significantly improves the generalizability and accuracy of the object detection model (Eversberg & Lambrecht, 2021; Zoph et al., 2020).

Conclusion

1. The YOLOv8 model was effective for the detection of the yellow coral *Dendrophyllia cornigera* and the cup sponge *Phakellia ventilabrum*, two key species of the Cantabrian Sea circalittoral shelf rock.
2. A powerful and accurate tool was developed, within a pipeline, that allows automatic detection of target species from raw transect images of the circalittoral shelf by remotely operated vehicles (ROVs).
3. The results show that all three models (YOLOv7, YOLOv8 and Faster R-CNN) improve their performance when trained with data augmentation and that

YOLOv8 is the model that presents the best performance in terms of precision, recall and F1 for both confidence thresholds 0.5 and 0.6.

4. The implementation of this tool in the shelf area of the Aviles (ACS) and Capbreton Submarine Cannon Systems (CCS) allowed monitoring of these vulnerable marine ecosystems, with detailed density maps of target species indicating that the CCS rocky shelf presented the highest densities *D. cornigera* and *P. ventilabrum*.

5. The implementation of deep learning based technologies are an efficient and accurate methodology for sampling and monitoring sessile benthic populations. This is essential to support the protection and conservation of biodiversity in these ecosystems.

Acknowledgements

This research has been carried out within the scope of the Nature + LIFE INDEMARES (07/NAT/E/000732) and INTEMARES projects, partially funded by the LIFE+ "Nature and Biodiversity" call of the European Commission (LIFE15 IPE ES 012) and coordinated by the Biodiversity Foundation of the Spanish Ministry for Ecological Transition, with the participation of different scientific institutions and NGOs.

Bibliografía

Abad-Uribarren, A., Prado, E., Sierra, S., Cobo, A., Rodríguez-Basalo, A., Gómez-Ballesteros, M., & Sánchez, F. (2022). Deep learning-assisted high resolution mapping of vulnerable habitats within the Capbreton Canyon System, Bay of Biscay. Estuarine, Coastal and Shelf Science, 275(107957), 107957. https://doi.org/10.1016/j.ecss.2022.107957

Abdulghanı̇, A. M. A. G., & Menekşe Dalveren, G. G. (2022). Moving object detection in video with algorithms YOLO and faster R-CNN in different conditions. European Journal of Science and Technology. https://doi.org/10.31590/ejosat.1013049

Baena, I., Mallol, S., Rodríguez, N., Fraile-Nuez, E., Arrieta, J. M., González-Vega, A., Vázquez, J.-T., Palomino, D., Díez, I. P., García, J., Ramos, J. M., Sánchez, F., Rodríguez, J. M., & Díaz., D. (2021). LIFE IP INTEMARES, Informe de la campaña INTEMARES_COLCARTO_0221. https://intemares.es/sites/default/files/informe_campana_columbretes_2021.pdf

Bhandarkar, S. M., Kathirvelu, S., & Hopkinson, B. M. (2022). Object detection in 3D coral ecosystem maps from multiple image sequences. 2022 26th International Conference on Pattern Recognition (ICPR).

BOE.es (1992). DOUE-L-1992-81200 Directiva 92/43/CEE del Consejo, de 21 de mayo de 1992, relativa a la conservación de los hábitats naturales y de la fauna y flora silvestres. (s/f). Boe.es. Recuperado el 16 de mayo de 2023, de https://www.boe.es/buscar/doc.php?id=DOUE-L-1992-81200

Bochkovskiy, A., Wang, C.-Y., & Liao, H.-Y. M. (2022). YOLOv7: Trainable bag-of-freebies sets new state-of-the-art for real-time object detectors. ArXiv, abs/2207.02696.

Dominguez-Carrió, C., Riera, J. L., Robert, K., Zabala, M., Requena, S., Gori, A., Orejas, C., Lo Iacono, C., Estournel, C., Corbera, G., Ambroso, S., Uriz, M. J., López-González, P. J., Sardá, R., & Gili, J.-M. (2022). Diversity, structure and spatial distribution of megabenthic communities in Cap de Creus continental shelf and submarine canyon (NW Mediterranean). Progress in Oceanography, 208(102877), 102877. https://doi.org/10.1016/j.pocean.2022.102877

Ercilla, G., Casas, D., Estrada, F., Vázquez, J. T., Iglesias, J., García, M., Gómez, M., Acosta, J., Gallart, J., & Maestro-González, A. (2008). Morphosedimentary features and recent depositional architectural model of the Cantabrian continental margin. Marine Geology, 247(1–2), 61–83. https://doi.org/10.1016/j.margeo.2007.08.007

Eversberg, L., & Lambrecht, J. (2021). Generating images with physics-based rendering for an industrial object detection task: Realism versus domain randomization. Sensors (Basel, Switzerland), 21(23), 7901. https://doi.org/10.3390/s21237901

FAO, 2009. International Guidelines for the Management of Deep-Sea Fisheries in the High-Seas. Food and Agriculture Organization of the United Nations, Rome.

flying-objects: Research app to generate synthetic data for detection / segmentation / instance segmentation tasks. (s/f). Github.com. Recuperado el 4 de Agosto de 2023, de https://github.com/supervisely-ecosystem/flying-objects

Karmaker, A., & Ray, P. (2023). A Comprehensive Review of YOLO: From YOLOv1 to YOLOv8 and Beyond. ArXiv, abs/2304.00501.

Kirillov, A., Mintun, E., Ravi, N., Mao, H., Rolland, C., Gustafson, L., Xiao, T., Whitehead, S., Berg, A. C., Lo, W.-Y., Dollár, P., & Girshick, R. (2023). Segment Anything. https://doi.org/10.48550/ARXIV.2304.02643

Knausgård, K. M., Wiklund, A., Sørdalen, T. K., Halvorsen, K. T., Kleiven, A. R., Jiao, L., & Goodwin, M. (2022). Temperate fish detection and classification: a deep learning based approach. Applied Intelligence, 52(6), 6988–7001. https://doi.org/10.1007/s10489-020-02154-9

Lamarck, J.-B. M. (1816). Histoire naturelle des animaux sans vertèbres. Tome second. Verdière. 568 pp

LeCun, Y., Bengio, Y., & Hinton, G. (2015). Deep learning. Nature, 521(7553), 436–444. https://doi.org/10.1038/nature14539

Li, J., Xu, W., Deng, L., Xiao, Y., Han, Z., & Zheng, H. (2022). Deep learning for visual recognition and detection of aquatic animals: A review. Reviews in Aquaculture. https://doi.org/10.1111/raq.12726

Linnaeus, C. (1766). Systema naturae per regna tria naturae: secundum classes, ordines, genera, species, cum characteribus, differentiis, synonymis, locis. Ed, 533–1327.

Liu, Y., & Wang, S. (2022). Corrigendum to “A quantitative detection algorithm based on improved faster R-CNN for marine benthos”. Ecological Informatics, 70(101655), 101655. https://doi.org/10.1016/j.ecoinf.2022.101655

Mahmood, A., Bennamoun, M., An, S., Sohel, F., Boussaid, F., Hovey, R., Kendrick, G., & Fisher, R. B. (2017). Deep learning for coral classification. En Handbook of Neural Computation (pp. 383–401). Elsevier.

Maity, M., Banerjee, S., & Sinha Chaudhuri, S. (2021). Faster R-CNN and YOLO based Vehicle detection: A Survey. 2021 5th International Conference on Computing Methodologies and Communication (ICCMC).

Olden, J. D., Lawler, J. J., & Poff, N. L. (2008). Machine learning methods without tears: a primer for ecologists. The Quarterly Review of Biology, 83(2), 171–193. https://doi.org/10.1086/587826

Pinheiro, M., Martins, I., Raimundo, J., Caetano, M., Neuparth, T., & Santos, M. M. (2023). Stressors of emerging concern in deep-sea environments: microplastics, pharmaceuticals, personal care products and deep-sea mining. The Science of the Total Environment, 876(162557), 162557. https://doi.org/10.1016/j.scitotenv.2023.162557

Prado, E., Rodríguez-Basalo, A., Cobo, A., Ríos, P., & Sánchez, F. (2020). 3D fine-scale terrain variables from underwater photogrammetry: A new approach to benthic microhabitat modeling in a circalittoral rocky shelf. Remote Sensing, 12(15), 2466. https://doi.org/10.3390/rs12152466

Raphael, A., Dubinsky, Z., Iluz, D., & Netanyahu, N. S. (2020). Neural Network recognition of marine benthos and corals. Diversity, 12(1), 29. https://doi.org/10.3390/d12010029

Redmon, J., Divvala, S., Girshick, R., & Farhadi, A. (2016). You only look once: Unified, real-time object detection. 2016 IEEE Conference on Computer Vision and Pattern Recognition (CVPR).

Ren, S., He, K., Girshick, R., & Sun, J. (2017). Faster R-CNN: Towards real-time object detection with region proposal networks. IEEE Transactions on Pattern Analysis and Machine Intelligence, 39(6), 1137–1149. https://doi.org/10.1109/TPAMI.2016.2577031

Ríos, P., Altuna, Á., Frutos, I., Manjón-Cabeza, E., García-Guillén, L., Macías-Ramírez, A., Ibarrola, T. P., Gofas, S., Taboada, S., Souto, J., Álvarez, F., Saiz-Salinas, J. I., Cárdenas, P., Rodríguez-Cabello, C., Lourido, A., Boza, C., Rodríguez-Basalo, A., Prado, E., Abad-Uribarren, A., … Cristobo, J. (2022). Avilés Canyon System: Increasing the benthic biodiversity knowledge. Estuarine, Coastal and Shelf Science, 274(107924), 107924. https://doi.org/10.1016/j.ecss.2022.107924

Rodríguez-Basalo, A., Ríos, P., Arrese, B., Abad-Uribarren, A., Cristobo, J., Ibarrola, T. P., Gómez-Ballesteros, M., Prado, E., & Sánchez, F. (2022). Mapping the habitats of a complex circalittoral rocky shelf in the Cantabrian Sea (South Bay of Biscay). Estuarine, Coastal and Shelf Science, 273(107912), 107912. https://doi.org/10.1016/j.ecss.2022.107912

Sánchez, F., & Rodríguez, J.M. (2013). POLITOLANA, a new low cost towed vehicle designed for the characterization of the deep-sea floor. Instrumentation Viewpoint. 69.

Schmidhuber, J. (2014). Deep learning in neural networks: An overview. En arXiv [cs.NE]. http://arxiv.org/abs/1404.7828

Schmidt, C., Muñoz, G., Lancaster, L. T., Lessard, J.-P., Marske, K. A., Marshall, K. E., & Garroway, C. J. (2022). Population demography maintains biogeographic boundaries. Ecology Letters, 25(8), 1905–1913. https://doi.org/10.1111/ele.14058

Siddiqui, S. A., Salman, A., Malik, M. I., Shafait, F., Mian, A., Shortis, M. R., & Harvey, E. S. (2018). Automatic fish species classification in underwater videos: exploiting pre-trained deep neural network models to compensate for limited labeled data. ICES Journal of Marine Science: Journal Du Conseil, 75(1), 374–389. https://doi.org/10.1093/icesjms/fsx109

Schoening, T., Bergmann, M., Ontrup, J., Taylor, J., Dannheim, J., Gutt, J., Purser, A., & Nattkemper, T. W. (2012). Semi-automated image analysis for the assessment of megafaunal densities at the Arctic deep-sea observatory HAUSGARTEN. PloS One, 7(6), e38179. https://doi.org/10.1371/journal.pone.0038179

Song, P., Li, P., Dai, L., Wang, T., & Chen, Z. (2022). Boosting R-CNN: Reweighting R-CNN samples by RPN's error for underwater object detection. https://doi.org/10.48550/ARXIV.2206.13728

Supervisely: unified OS for computer vision. (s/f). Supervisely.com. Recuperado el 26 de Abril de 2023, de https://supervisely.com/

Van Rijsbergen, C. J. (1974). Foundation of evaluation. The Journal of Documentation; Devoted to the Recording, Organization and Dissemination of Specialized Knowledge, 30(4), 365–373. https://doi.org/10.1108/eb026584

Wang, N., Liu, H., Li, Y., Zhou, W., & Ding, M. (2023). Segmentation and phenotype calculation of rapeseed pods based on YOLO v8 and Mask R-convolution neural networks. Plants, 12(18). https://doi.org/10.3390/plants12183328

Weinstein, B. G. (2018). A computer vision for animal ecology. The Journal of Animal Ecology, 87(3), 533–545. https://doi.org/10.1111/1365-2656.12780

Weinstein, B. G., Garner, L., Saccomanno, V. R., Steinkraus, A., Ortega, A., Brush, K., Yenni, G., McKellar, A. E., Converse, R., Lippitt, C. D., Wegmann, A., Holmes, N. D., Edney, A. J., Hart, T., Jessopp, M. J., Clarke, R. H., Marchowski, D., Senyondo, H., Dotson, R., … Ernest, S. K. M. (2022). A general deep learning model for bird detection in high-resolution airborne imagery. Ecological Applications: A Publication of the Ecological Society of America, 32(8), e2694. https://doi.org/10.1002/eap.2694

Xu, W., & Matzner, S. (2018). Underwater fish detection using deep learning for water power applications. 2018 International Conference on Computational Science and Computational Intelligence (CSCI).

Xu, X., Liu, Y., Lyu, L., Yan, P., & Zhang, J. (2023). MAD-YOLO: A quantitative detection algorithm for dense small-scale marine benthos. Ecological Informatics, 75(102022), 102022. https://doi.org/10.1016/j.ecoinf.2023.102022

Zhang, J., Yongpan, W., Xianchong, X., Yong, L., Lyu, L., & Wu, Q. (2022). YoloXT: A object detection algorithm for marine benthos. Ecological Informatics, 72(101923), 101923. https://doi.org/10.1016/j.ecoinf.2022.101923

Zhong, J., Li, M., Qin, J., Cui, Y., Yang, K., & Zhang, H. (2022). Real-time marine animal detection using Yolo-based deep learning networks in the coral reef ecosystem. ISPRS - International Archives of the Photogrammetry Remote Sensing and Spatial Information Sciences, XLVI-3/W1-2022, 301–306. https://doi.org/10.5194/isprs-archives-xlvi-3-w1-2022-301-2022

Zoph, B., Cubuk, E. D., Ghiasi, G., Lin, T.-Y., Shlens, J., & Le, Q. V. (2020). Learning data augmentation strategies for object detection. En Computer Vision – ECCV 2020 (pp. 566–583). Springer International Publishing.

Table 1(on next page)

Impact of Data Augmentation on Object Detection Model Performance for *D. cornigera* and *P. ventilabrum*

Difference in performance of YOLOv8, YOLOv7 and Faster R-CNN models in terms of precision, recall and F1 for *D. cornigera* and *P. vetilabrum* species with and without data augmentation. Values represent the difference between model performance with data augmentation minus model performance without data augmentation.

	D. cornigera			*P. ventilabrum*		
Model	**Precision (%)**	**Recall (%)**	**F1 (%)**	**Precision (%)**	**Recall (%)**	**F1 (%)**
YOLOv8	1,4	18,5	11,4	5,7	3,5	3,3
YOLOv7	7,7	10,4	9,6	0,5	3,1	2,3
Faster R-CNN	0,4	1,6	1,5	3,5	8,5	5,2

Figure 1

Geographical and Bathymetric Overview of Study Areas in the Cantabrian Sea

(A) Location map showing the study areas highlighted by a green rectangle, located in the Cantabrian Sea. In addition, detailed representations of the bathymetry of (B) the Aviles submarine canyon system and (C) the Capbreton submarine canyon system are presented, where the ROV transects identified by red dots are highlighted.

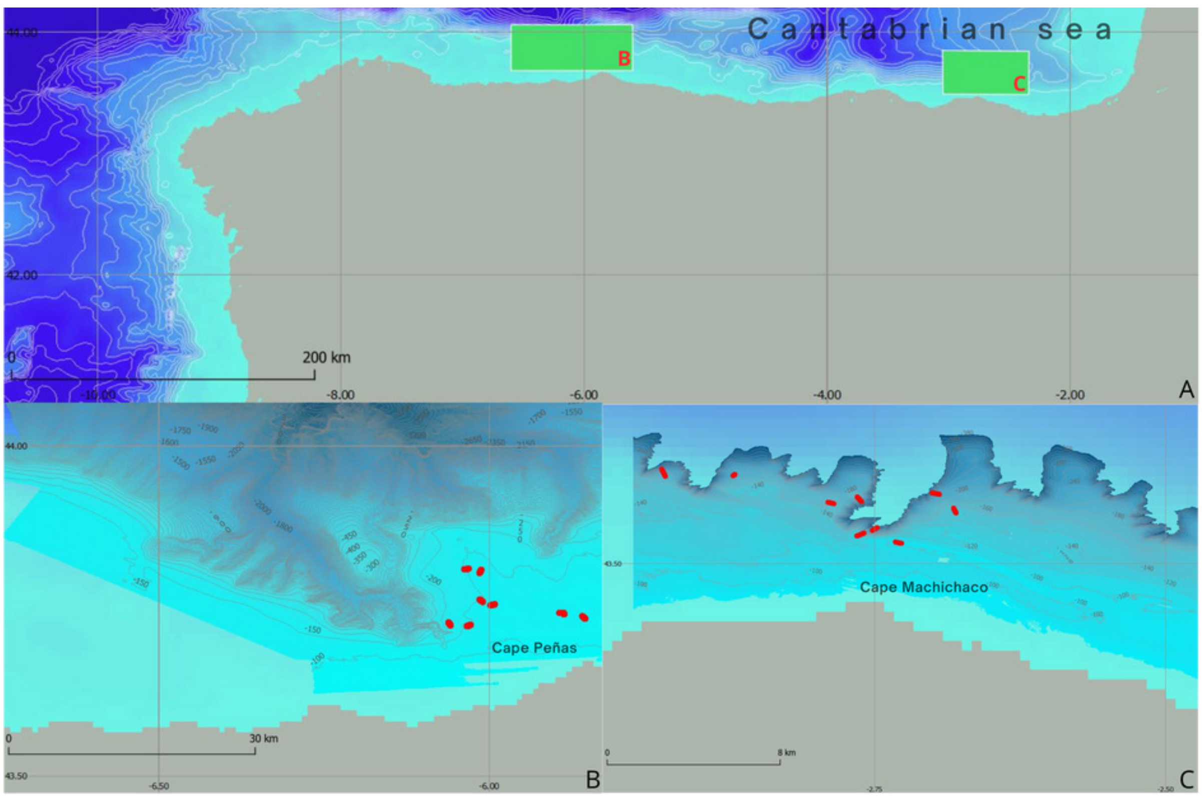

Figure 2

Detailed Photographs of *Dendrophyllia cornigera* and *Phakellia ventilabrum*

Detailed photograph of the species (A) *Dendrophyllia cornigera* and (B) *Phakellia ventilabrum*.

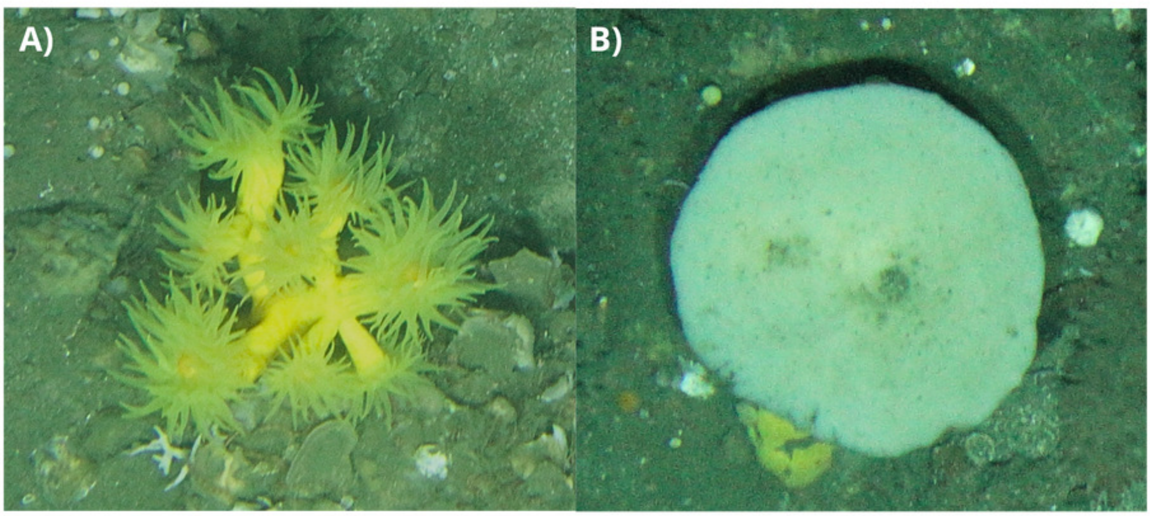

Figure 3

ROTV Captured Images of Marine Species in Capbreton and Aviles Canyon Systems

ROTV-obtained images of marine species on rocky substrate. (A) Capbreton canyon system, showing *Dendrophyllia cornigera* (Dc), *Phakellia ventilabrum* (Pv), encrusting sponges (Ei), other Porifera organisms (Po), *Viminella flagellum* coral (Vf), and *Filograna cf implexa* serpulid (Fi). (B) Aviles canyon system, displaying Dc, Pv, Ei, At, Po, *Leptometra celtica* (Lc), *Parastichopus regalis* (Pr), and *Gracilechinus acutus* urchin (Ga). Lasers are visible in the center of both images.

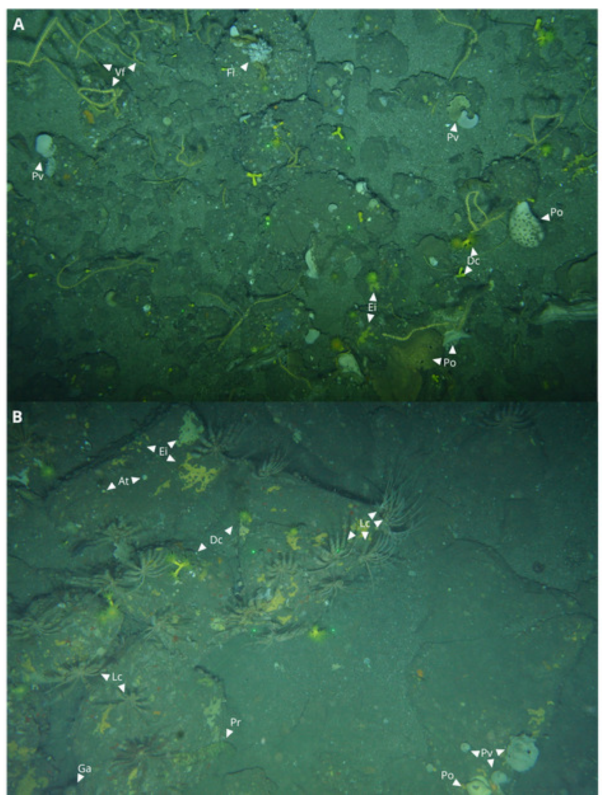

Figure 4

Synthetic Image Generation of *D. cornigera* and *P. ventilabrum* Using Supervisely

Synthetic images generated using Supervisely image data annotation software. (A) Specimens of both *D. cornigera* and *P. ventilabrum*. (B) Specimens of *D. cornigera* only. (C) Specimens of *P. ventilabrum* only. Each image, enhanced by the flying object function for magnification and sample size increase, contains an average of 120 annotations.

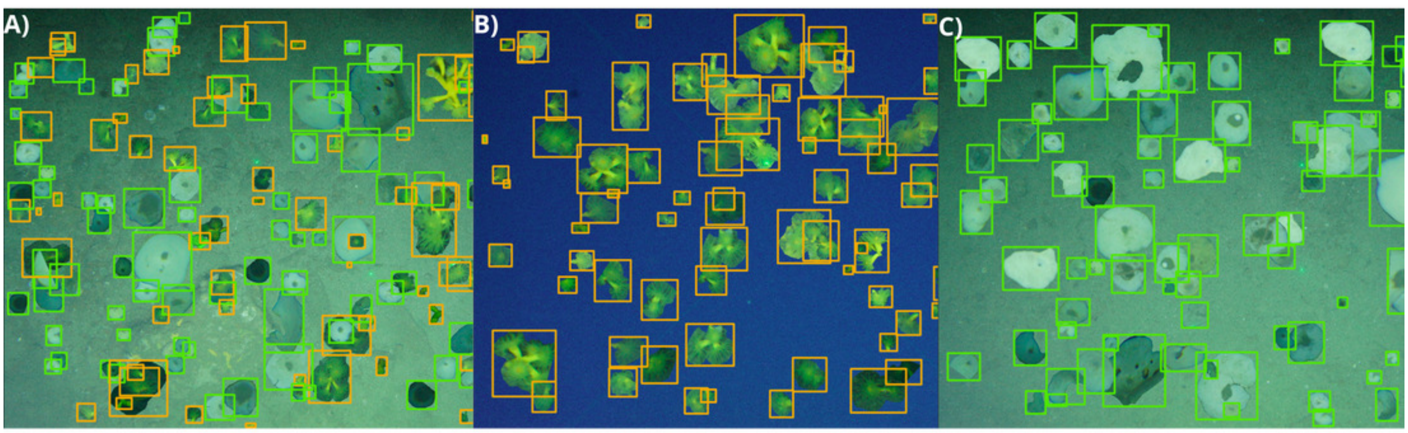

Figure 5

Intersection Over Union (IoU) Calculation for *D. cornigera* Detection

The image shows the calculation of the intersection over union (IoU) for the detection of *D. cornigera.* Orange (A) shows the bounding box of the annotation and blue (B) shows the bounding box of the inference, as well as the center of each box and the distance between both points. The IoU is calculated as the intersection between the two boxes divided by their junction.

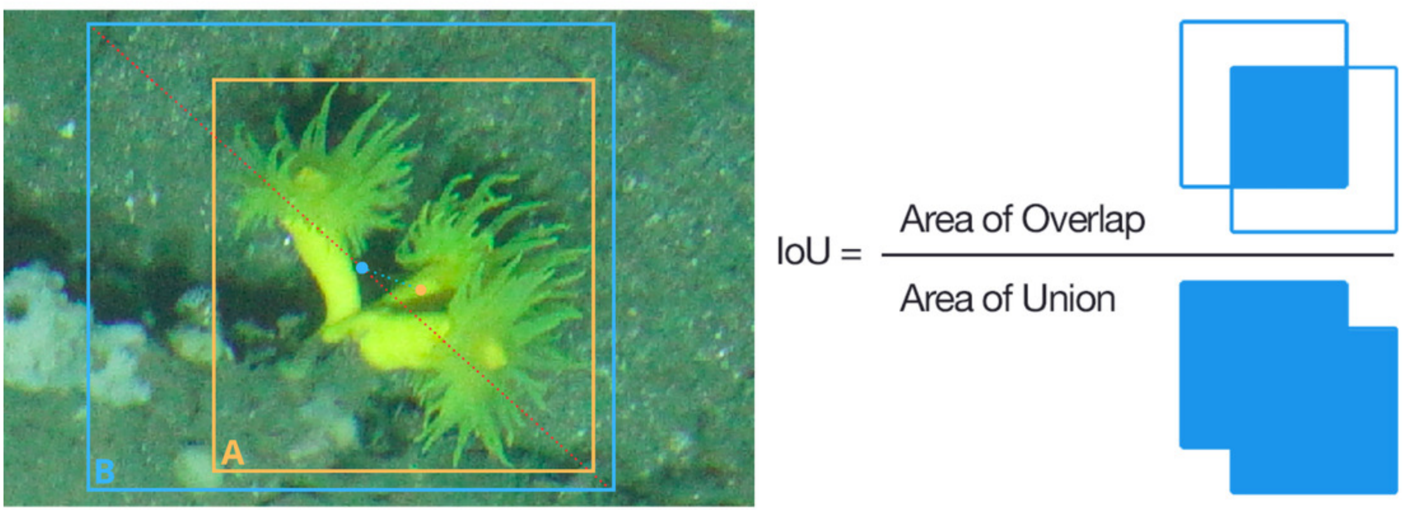

Figure 6

Automated Species Density Map Generation Pipeline in Google Colab

Graphical representation of the pipeline implemented in Google Colab for automated generation of species density maps from raw transect images and ROTV telemetry data.

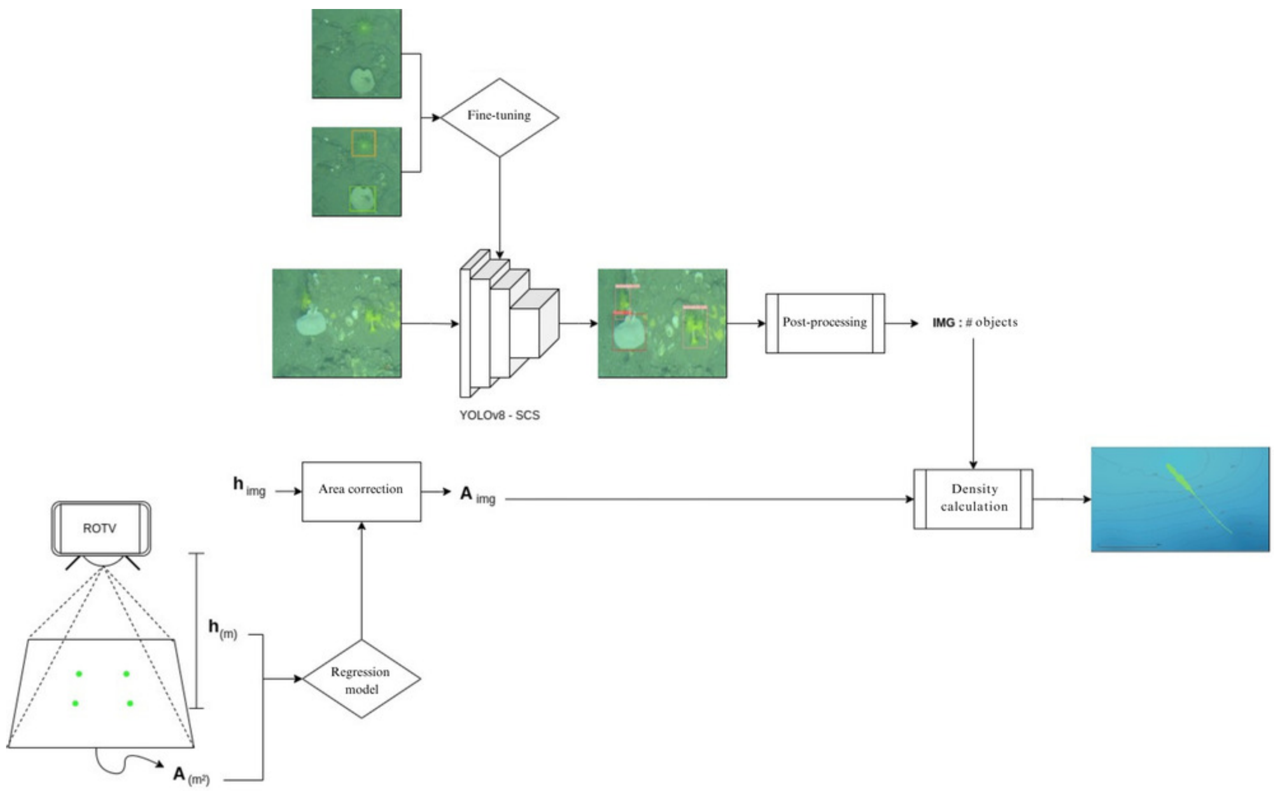

Figure 7

Metrics Comparison for Species Detection Using YOLOv8, YOLOv7 and Faster R-CNN Models

Comparison of metrics for detection of *P. ventilabrum* and *D. cornigera* species using the YOLOv8, YOLOv7 and Faster R-CNN models in the ACS and CCS. precision, recall and F1 metrics were analyzed using augmented data and confidence thresholds of 0.5 and 0.6.

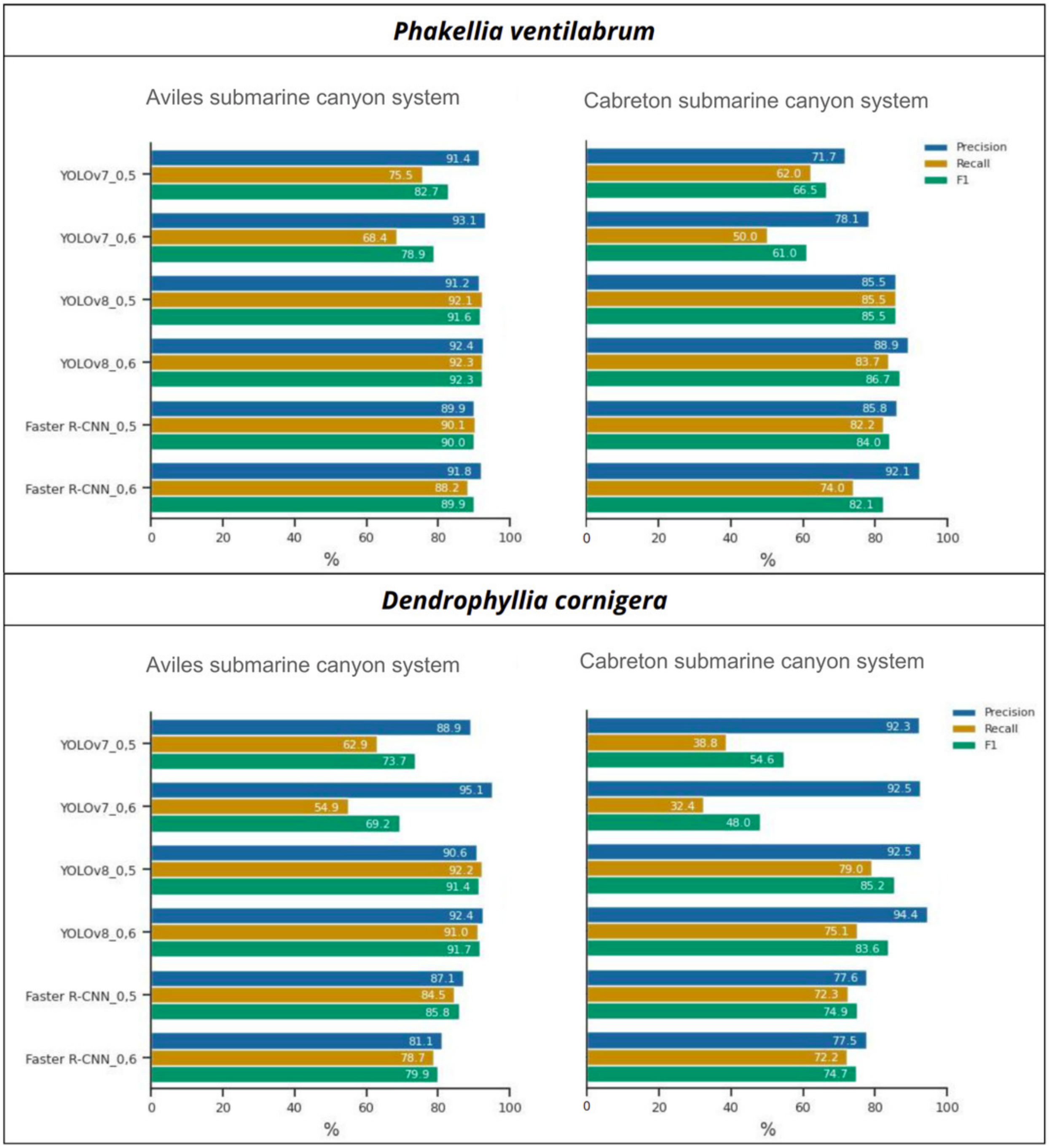
Phakellia ventilabrum
Aviles submarine canyon system
Cabreton submarine canyon system
Precision
Recall
F1
YOLOv7_0,5
YOLOv7_0,6
YOLOv8_0,5
YOLOv8_0,6
Faster R-CNN_0,5
Faster R-CNN_0,6
91.4
75.5
82.7
93.1
68.4
78.9
91.2
92.1
91.6
92.4
92.3
92.3
89.9
90.1
90.0
91.8
88.2
89.9
71.7
62.0
66.5
78.1
50.0
61.0
85.5
85.5
85.5
88.9
83.7
86.7
85.8
82.2
84.0
92.1
74.0
82.1
%
Dendrophyllia cornigera
Aviles submarine canyon system
Cabreton submarine canyon system
88.9
62.9
73.7
95.1
54.9
69.2
90.6
92.2
91.4
92.4
91.0
91.7
87.1
84.5
85.8
81.1
78.7
79.9
92.3
38.8
54.6
92.5
32.4
48.0
92.5
79.0
85.2
94.4
75.1
83.6
77.6
72.3
74.9
77.5
72.2
74.7
%

Figure 8

Detection Results Comparison of Different Algorithms for CCS Images

Comparison of detection results of different algorithms for images obtained from the CCS. (A) and (B) represent different images. Red circles indicate false detections, while blue circles indicate missed detections. The detection model used is shown in the right frame of each image.

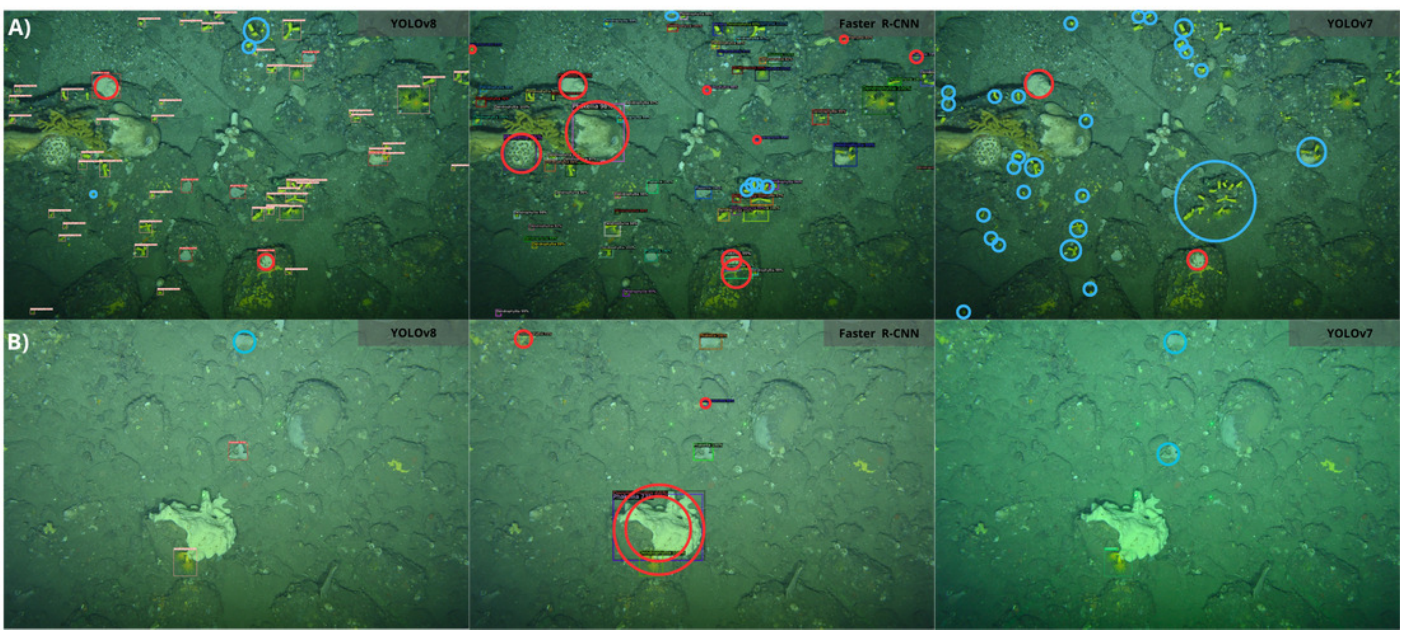

Figure 9

Species Density Maps for *D. cornigera* and *P. ventilabrum* in Aviles and Capbreton Canyon Systems

Species density maps for (A) *Dendrophyllia cornigera* and (B) *Phakellia ventilabrum*. Both species are shown in the Aviles Submarine Canyon System (bottom left) and the Capbreton Canyon System (bottom right). A large-scale situation map at the top depicts the locations of both canyon systems.